Available online at www.sciencedirect.com

ScienceDirect

Procedia Computer Science 108C (2017) 2373–2377

Procedia Computer Science

International Conference on Computational Science, ICCS 2017, 12-14 June 2017, Zurich, Switzerland

Classification of Critical Points Using a Second Order Derivative

Michal Smolik[1] and Vaclav Skala[1]
[1] *University of West Bohemia, Plzen, Czech Republic*
{smolik, skala}@kiv.zcu.cz

Abstract
This article presents a new method for classification of critical points. A vector field is usually classified using only a Jacobian matrix of the approximated vector field. This work shows how an approximation using a second order derivative can be used for more detailed classification. An algorithm for calculation of the curvature of main axes is also presented.

Peer-review under responsibility of the scientific committee of the International Conference on Computational Science

Keywords: vector field; critical point; Hessian matrix; curvature

1 Introduction

The visualization of vector field topology is a problem that arises naturally when studying the qualitative structure of flows. The knowledge of the data at a single point would be of little help when the goal is to obtain knowledge and understanding of the whole vector field. The individual numbers can be of little interest. It is the connection between them which is important.

Helman and Hesselink [1] introduced the concept of the topology of a planar vector field to the visualization community. They extracted critical points and classified them into sources, sinks and saddles, and integrated certain stream lines called separatrices from the saddles in the directions of the eigenvectors of the Jacobian matrix. Later, topological methods have been extended to higher order critical points [6], boundary switch points [3], and closed separatrices [14]. In addition, topological methods using classification have been applied to simplify [7], smooth and compress [2] vector fields.

Theisel [10] presents a summary of vector field curvatures. Weinkauf and Theisel [12] present the theory of curvature measures of $3D$ vector fields. The curvature measurements are used to measure the distance between streamlines in vector fields [4].

All of the published research uses for classification of critical points and vector field description only linear approximation of the vector field. None of it uses an approximation with second order partial derivatives, i.e. a Hessian matrix. This approximation gives a more detailed description of the vector field around a critical point and can be used for a more detailed classification. Use of an approximation with a Hessian matrix will be described in this paper.

Peer-review under responsibility of the scientific committee of the International Conference on Computational Science
10.1016/j.procs.2017.05.271

2 Approximation Using a Hessian Matrix

Vector fields are approximated using only linear approximation to determine the local behavior of the vector field [1]. However, linearization gives us only a basic classification of the critical points and basic information about the flow around them; the approximation using second order derivatives will give us some more information.

An approximation of the vector field around a critical point using a second order derivative must be written for each vector component (v_x and v_y) separately; see the following equation for v_x:

$$v_x = \begin{bmatrix} \frac{\partial v_x}{\partial x} \\ \frac{\partial v_x}{\partial y} \end{bmatrix}^T \cdot \begin{bmatrix} \Delta x \\ \Delta y \end{bmatrix} + \frac{1}{2} \begin{bmatrix} \Delta x \\ \Delta y \end{bmatrix}^T \cdot \begin{bmatrix} \frac{\partial^2 v_x}{\partial x^2} & \frac{\partial^2 v_x}{\partial x \partial y} \\ \frac{\partial^2 v_x}{\partial y \partial x} & \frac{\partial^2 v_x}{\partial y^2} \end{bmatrix} \cdot \begin{bmatrix} \Delta x \\ \Delta y \end{bmatrix} = \boldsymbol{J}_x \cdot \Delta \boldsymbol{x} + \frac{1}{2} \Delta \boldsymbol{x}^T \cdot \boldsymbol{H}_x \cdot \Delta \boldsymbol{x} \tag{1}$$

where $\Delta x = x - x_0$, $\Delta y = y - y_0$, $\Delta \boldsymbol{x} = [\Delta x, \Delta y]^T$, $\boldsymbol{H}_x$ is Hessian matrix, $\boldsymbol{J}_x$ is the first row of a Jacobian matrix. Equation for v_y is similar as for v_x.

A Hessian matrix is a square matrix of second-order partial derivatives of a scalar-valued function, or scalar field. It describes the local curvature of a function of many variables.

An approximation of a vector field using (1) is a bit more computationally expensive than the standard linear approximation, but gives us a more detailed description than a linear approximation of a vector field, see Fig. 2. The approximation in Fig. 2 ($t \neq 0$) gives us the same information as in Fig. 2 ($t = 0$), although we can see the curvature of the two main axes for the saddle.

3 Curvature of a Vector Field

An approximated vector field using (1) is not only linear but contains the Hessian matrices that describe the local curvature of the vector field. In this section, an approach for computing the local curvature of a vector field that is approximated with Jacobian and Hessian matrices is introduced.

Using an approximation of the vector field with second order derivatives gives us the opportunity to compute a Jacobian matrix $\boldsymbol{J}_\varepsilon$ in the neighborhood of a critical point from approximated vector field (1):

$$\boldsymbol{J}_\varepsilon = \begin{bmatrix} \left.\frac{\partial v_x}{\partial x}\right|_{\boldsymbol{x}_0+\boldsymbol{\varepsilon}} & \left.\frac{\partial v_x}{\partial y}\right|_{\boldsymbol{x}_0+\boldsymbol{\varepsilon}} \\ \left.\frac{\partial v_y}{\partial x}\right|_{\boldsymbol{x}_0+\boldsymbol{\varepsilon}} & \left.\frac{\partial v_y}{\partial y}\right|_{\boldsymbol{x}_0+\boldsymbol{\varepsilon}} \end{bmatrix}, \tag{2}$$

where $\boldsymbol{\varepsilon} = \left[e_x, e_y\right]^T$ is an arbitrary direction vector pointing from the critical point $\boldsymbol{x}_0$. The matrix $\boldsymbol{J}_{\boldsymbol{\varepsilon}}$ (2×2) in (2) can be rewritten using elements of $\boldsymbol{J}$, $\boldsymbol{H}_x$ (1) and $\boldsymbol{H}_y$ as:

$$\left[\begin{array}{c:c} \left.\frac{\partial v_x}{\partial x}\right|_{\boldsymbol{x}_0} + \left.\frac{\partial^2 v_x}{\partial x^2}\right|_{\boldsymbol{x}_0} \varepsilon_x + \frac{1}{2}\left(\left.\frac{\partial^2 v_x}{\partial x \partial y}\right|_{\boldsymbol{x}_0} + \left.\frac{\partial^2 v_x}{\partial y \partial x}\right|_{\boldsymbol{x}_0}\right)\varepsilon_y & \left.\frac{\partial v_x}{\partial y}\right|_{\boldsymbol{x}_0} + \left.\frac{\partial^2 v_x}{\partial y^2}\right|_{\boldsymbol{x}_0} \varepsilon_x + \frac{1}{2}\left(\left.\frac{\partial^2 v_x}{\partial x \partial y}\right|_{\boldsymbol{x}_0} + \left.\frac{\partial^2 v_x}{\partial y \partial x}\right|_{\boldsymbol{x}_0}\right)\varepsilon_x \\ \hdashline \left.\frac{\partial v_y}{\partial x}\right|_{\boldsymbol{x}_0} + \left.\frac{\partial^2 v_y}{\partial x^2}\right|_{\boldsymbol{x}_0} \varepsilon_x + \frac{1}{2}\left(\left.\frac{\partial^2 v_y}{\partial x \partial y}\right|_{\boldsymbol{x}_0} + \left.\frac{\partial^2 v_y}{\partial y \partial x}\right|_{\boldsymbol{x}_0}\right)\varepsilon_y & \left.\frac{\partial v_y}{\partial y}\right|_{\boldsymbol{x}_0} + \left.\frac{\partial^2 v_y}{\partial y^2}\right|_{\boldsymbol{x}_0} \varepsilon_x + \frac{1}{2}\left(\left.\frac{\partial^2 v_y}{\partial x \partial y}\right|_{\boldsymbol{x}_0} + \left.\frac{\partial^2 v_y}{\partial y \partial x}\right|_{\boldsymbol{x}_0}\right)\varepsilon_x \end{array}\right]. \tag{3}$$

Assuming that $\boldsymbol{v}$ has continuous second partial derivatives at any given point, the mixed derivatives of v_x and v_y in the Hessian matrix are commutative. Equation (3) can be simplified and rewritten as

$$\boldsymbol{J}_\varepsilon = \begin{bmatrix} \left.\frac{\partial v_x}{\partial x}\right|_{\boldsymbol{x}_0} & \left.\frac{\partial v_x}{\partial y}\right|_{\boldsymbol{x}_0} \\ \left.\frac{\partial v_y}{\partial x}\right|_{\boldsymbol{x}_0} & \left.\frac{\partial v_y}{\partial y}\right|_{\boldsymbol{x}_0} \end{bmatrix} + \begin{bmatrix} \left.\frac{\partial^2 v_x}{\partial x^2}\right|_{\boldsymbol{x}_0} & \left.\frac{\partial^2 v_x}{\partial x \partial y}\right|_{\boldsymbol{x}_0} \\ \left.\frac{\partial^2 v_y}{\partial x^2}\right|_{\boldsymbol{x}_0} & \left.\frac{\partial^2 v_y}{\partial x \partial y}\right|_{\boldsymbol{x}_0} \end{bmatrix} \varepsilon_x + \begin{bmatrix} \left.\frac{\partial^2 v_x}{\partial x \partial y}\right|_{\boldsymbol{x}_0} & \left.\frac{\partial^2 v_x}{\partial y^2}\right|_{\boldsymbol{x}_0} \\ \left.\frac{\partial^2 v_y}{\partial x \partial y}\right|_{\boldsymbol{x}_0} & \left.\frac{\partial^2 v_y}{\partial y^2}\right|_{\boldsymbol{x}_0} \end{bmatrix} \varepsilon_y \tag{4}$$

Elements of $\boldsymbol{J}$, $\boldsymbol{H}_x$ (1) and $\boldsymbol{H}_y$ are all elements used to calculate $\boldsymbol{J}_\varepsilon$ in (3) and (4), so there is no need to compute any additional derivatives than those in (1). Note that the Jacobian matrix $\boldsymbol{J}_\varepsilon$ is for $\boldsymbol{\varepsilon} = [0,0]^T$ equal to Jacobian matrix $\boldsymbol{J}$. The Jacobian matrix $\boldsymbol{J}_\varepsilon$ can be computed for any point $(\boldsymbol{x_0} + \boldsymbol{\varepsilon})$. Therefore, we start by computing the eigenvectors of Jacobian matrix $\boldsymbol{J}$ in a critical point $\boldsymbol{x}_0$.

There are two eigenvectors ($\boldsymbol{u}_1$ and $\boldsymbol{u}_2$) for a Jacobian matrix in $2D$. In the case that the vector field is circular around the critical point, we will use only the real part of the eigenvectors, i.e.

$$\begin{matrix} Re(a+bi) = a \\ Im(a+bi) = b \end{matrix} \qquad a, b \in \mathbb{R}\,. \tag{5}$$

To calculate the curvature of the vector field we need to compute the eigenvectors in the near surroundings of the critical point as will be explained later. First, we need to compute vectors pointing from $\boldsymbol{x}_0$ in the direction of the main axes of the vector field, i.e.

$$\boldsymbol{\varepsilon}_{1L} = -\frac{Re(\boldsymbol{u}_1)}{\|Re(\boldsymbol{u}_1)\|}h \quad \boldsymbol{\varepsilon}_{2L} = -\frac{Re(\boldsymbol{u}_2)}{\|Re(\boldsymbol{u}_2)\|}h \quad \boldsymbol{\varepsilon}_{1R} = \frac{Re(\boldsymbol{u}_1)}{\|Re(\boldsymbol{u}_1)\|}h \quad \boldsymbol{\varepsilon}_{2R} = \frac{Re(\boldsymbol{u}_2)}{\|Re(\boldsymbol{u}_2)\|}h\,, \tag{6}$$

where h is some small number (e.g. $h = 10^{-3}$ for the vector field in Fig. 2).

In the next step, we calculate Jacobian matrix $\boldsymbol{J}_\varepsilon$ for all vectors computed in (6), i.e. the Jacobian matrix at points $(\boldsymbol{x}_0 + \boldsymbol{\varepsilon}_{**})$:

$$\boldsymbol{J}_{1L} = \boldsymbol{J}_\varepsilon(\boldsymbol{\varepsilon}_{1L}) \qquad \boldsymbol{J}_{2L} = \boldsymbol{J}_\varepsilon(\boldsymbol{\varepsilon}_{2L}) \qquad \boldsymbol{J}_{1R} = \boldsymbol{J}_\varepsilon(\boldsymbol{\varepsilon}_{1R}) \qquad \boldsymbol{J}_{2R} = \boldsymbol{J}_\varepsilon(\boldsymbol{\varepsilon}_{2R})\,. \tag{7}$$

For each Jacobian matrix in (7) we need to calculate the real parts of both eigenvectors and determine which one is pointing in almost the same direction as the original eigenvector $Re(\boldsymbol{u}_1)$ for $\boldsymbol{J}_{1L}$ and $\boldsymbol{J}_{1R}$ and determine $\boldsymbol{u}_{1L}$ and $\boldsymbol{u}_{1R}$, respectively; similarly eigenvector $Re(\boldsymbol{u}_2)$ for $\boldsymbol{J}_{2L}$ and $\boldsymbol{J}_{2R}$ and determine $\boldsymbol{u}_{2L}$ and $\boldsymbol{u}_{2R}$. This test can be done using the dot product between original eigenvector $Re(\boldsymbol{u}_i)$, where $i = \{1, 2\}$, and both real parts of eigenvectors for Jacobian matrix $\boldsymbol{J}_{i*}$ in (7). The closest two vectors, i.e. vectors with a minimal angle between them, have the greatest dot product. Therefore, for each directional vector in (6) we get one vector, thus four vectors $\boldsymbol{u}_{1L}$, $\boldsymbol{u}_{1R}$, $\boldsymbol{u}_{2L}$ and $\boldsymbol{u}_{2R}$, i.e., for example, $\boldsymbol{u}_{1L}$ is computed as the following procedure:

$$\{{}^1\boldsymbol{\xi}_{1L}, {}^2\boldsymbol{\xi}_{1L}\} = Re\big(eigenvectors(\boldsymbol{J}_{1L})\big) \qquad \boldsymbol{u}_{1L} = \begin{cases} {}^1\boldsymbol{\xi}_{1L} & {}^1\boldsymbol{\xi}_{1L} \cdot Re(\boldsymbol{u}_1) > {}^2\boldsymbol{\xi}_{1L} \cdot Re(\boldsymbol{u}_1) \\ {}^2\boldsymbol{\xi}_{1L} & {}^1\boldsymbol{\xi}_{1L} \cdot Re(\boldsymbol{u}_1) > {}^2\boldsymbol{\xi}_{1L} \cdot Re(\boldsymbol{u}_1) \end{cases}. \tag{8}$$

The curvature vectors of a vector field are computed as follows:

$$\boldsymbol{c}_1 = \frac{1}{2h}\left(\frac{\boldsymbol{u}_{1R}}{\|\boldsymbol{u}_{1R}\|} - \frac{\boldsymbol{u}_{1L}}{\|\boldsymbol{u}_{1L}\|}\right) \qquad \boldsymbol{c}_2 = \frac{1}{2h}\left(\frac{\boldsymbol{u}_{2R}}{\|\boldsymbol{u}_{2R}\|} - \frac{\boldsymbol{u}_{2L}}{\|\boldsymbol{u}_{2L}\|}\right)\,. \tag{9}$$

This is a discrete formula for curvature calculation using the difference between two unit vectors. The important property of the curvature vectors in (9) is the perpendicularity to $Re(\boldsymbol{u}_1)$, resp. $Re(\boldsymbol{u}_2)$, i.e.

$$\boldsymbol{c}_1 \cdot Re(\boldsymbol{u}_1) = 0 \qquad \boldsymbol{c}_2 \cdot Re(\boldsymbol{u}_2) = 0\,. \tag{10}$$

The length of the curvature vectors in (9) is a number that characterizes how much each of the main axes of the vector field is curved. In the case that both curvatures are equal to zero, then matrices $\boldsymbol{H}_x$ and $\boldsymbol{H}_y$ must be zero matrices; otherwise at least one of the curvatures is nonzero.

4 Example of Vector Field Curvature

The vector field around a critical point can be classified as one of the vector types [1]. This section presents examples of how the vector field approximated with the same Jacobian matrix changes when changing the Hessian matrices used to approximate the vector field around a critical point.

An example of the vector field around a saddle point can be characterized with the following approximation:

$$\begin{aligned} v_x &= \begin{bmatrix}1.2\\1.4\end{bmatrix}^T \cdot \begin{bmatrix}\Delta x\\ \Delta y\end{bmatrix} + \frac{1}{2}t\begin{bmatrix}\Delta x\\ \Delta y\end{bmatrix}^T \cdot \begin{bmatrix}1.2 & 0.84\\ 0.84 & 1.2\end{bmatrix} \cdot \begin{bmatrix}\Delta x\\ \Delta y\end{bmatrix} \\ v_y &= \begin{bmatrix}0.7\\-0.9\end{bmatrix}^T \cdot \begin{bmatrix}\Delta x\\ \Delta y\end{bmatrix} + \frac{1}{2}t\begin{bmatrix}\Delta x\\ \Delta y\end{bmatrix}^T \cdot \begin{bmatrix}-2 & 0.6\\ 0.6 & 2\end{bmatrix} \cdot \begin{bmatrix}\Delta x\\ \Delta y\end{bmatrix}, \end{aligned} \tag{11}$$

where $t \in \mathbb{R}$ is a parameter. If we continuously change the parameter t, the vector field will change continuously as well, i.e. there will be no discontinuity.

As an example, the parameter $t \in \langle -1; 1 \rangle$ was changed and both curvatures of the main axes of the vector field were calculated. It can be seen that both the curvatures change continuously (see results in Fig. 1). For parameter $t = 0$, the vector field is approximated only with the Jacobian matrix part of (11), i.e.

$$v_x = [1.2 \quad 1.4] \cdot [\Delta x \quad \Delta y]^T \qquad\qquad v_y = [0.7 \quad -0.9] \cdot [\Delta x \quad \Delta y]^T \tag{12}$$

and both the curvatures are thus equal to 0.

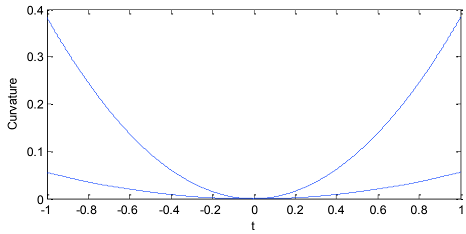

Fig. 1. Progress of both curvatures when changing parameter $t \in \langle -1; 1 \rangle$ in (11). One curvature grows faster with a greater absolute value of t. This means that one main axis is more curved than the other.

The approximated vector field represented by (11) can be seen for different values of parameter t in Fig. 2. It can be seen that the vector field has a different phase portrait for different values t; however, all of them have the same description using a linear approximation of the vector field around a critical point.

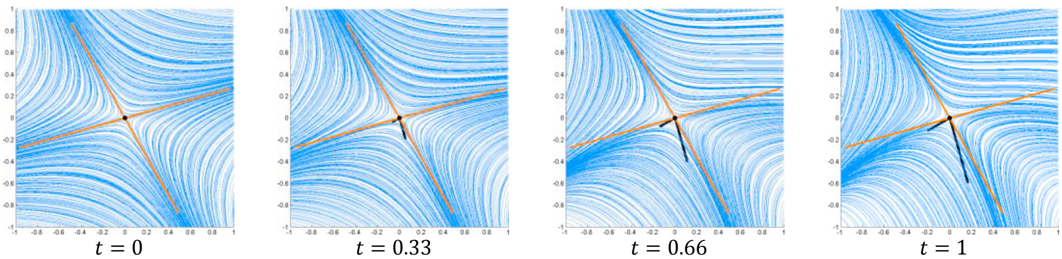

Fig. 2. Vector fields and their curvatures for different parameters t in (11). The orange lines visualize the main axes of vector fields obtained from the linear part of the approximation. The black lines visualize vectors of the curvature of the main axes (note that they are perpendicular to the main orange axes).

5 Conclusion

A new and easy algorithm for calculating the curvature of vector fields has been presented. It uses second order partial derivatives for an approximation of a vector field around a critical point. This approximation gives us a more detailed description of the vector field close to the critical point than the standardly used linear approximation.

The algorithm was presented for $2D$ flow fields because of their simplicity and clarity, but it can in general be used with no modifications for N dimensional vector flow fields.

Acknowledgments

The authors would like to thank their colleagues at the University of West Bohemia, Plzen, for their discussions and suggestions, and anonymous reviewers for their valuable comments and hints provided. The research was supported by projects Czech Science Foundation (GACR) No. 17-05534S and partly by SGS 2016-013.

References

[1] J. Helman and L. Hesselink. “Representation and display of vector field topology in fluid flow data sets,” IEEE Computer, Vol. 22, No. 8, pp. 27-36, 1989.

[2] S. Koch, J. Kasten, A. Wiebel, G. Scheuermann and M. Hlawitschka, “2D Vector field approximation using linear neighborhoods,” The Visual Computer, pp. 1-16, 2015.

[3] W. de Leeuw and R. van Liere, “Collapsing flow topology using area metrics,” Proc. IEEE Visualization ’99, pp. 349-354, 1999.

[4] K. Lu, A. Chaudhuri, T. Y. Lee, H. W. Shen and P. C. Wong. “Exploring vector fields with distribution-based streamline analysis,” PacificVis, pp. 257-264, 2013.

[5] P. A. Philippou, and R. N. Strickland, “Vector field analysis and synthesis using three dimensional phase portraits,” Graph. Models Image Process., Vol. 59, No. 6, pp. 446-462, 1997.

[6] G. Scheuermann, H. Krüger, M. Menzel, and A. Rockwood, “Visualizing non-linear vector field topology,” IEEE Transactions on Visualization and Computer Graphics, Vol. 4, No. 2, pp. 109-116, 1998.

[7] P. Skraba, B. Wang, G. Chen, and P. Rosen, ”2D vector field simplification based on robustness,” Pacific Visualization Symposium (PacificVis), IEEE, pp. 49-56, 2014.

[8] M. Smolik, V. Skala, “Spherical RBF Vector Field Interpolation: Experimental Study,” SAMI 2017, pp. 431-434, Slovakia, 2017.

[9] M. Smolik, V. Skala, “Vector Field Interpolation with Radial Basis Functions,” SIGRAD 2016, pp. 15-21, Sweden, 2016

[10] H. Theisel, “Vector field curvature and applications,” PhD dissertation, University of Rostock, Germany, 1995.

[11] US GFS global weather model. National Centers for Environmental Information (NCEI), https://www.ncdc.noaa.gov/data-access/model-data/model-datasets/global-forcast-system-gfs, [downloaded: 9.11.2016].

[12] T. Weinkauf and H. Theisel. “Curvature measures of 3D vector fields and their applications”, Journal of WSCG, Vol. 10, No. 2, 2002.

[13] T. Weinkauf, H. Theisel, K. Shi, H.-C. Hege, and H.-P. Seidel, “Extracting higher order critical points and topological simplification of 3D vector fields,” Proc. IEEE Visualization 2005, pp. 559-566, Minneapolis, U.S.A., 2005.

[14] T. Wischgoll and G. Scheuermann, “Detection and visualization of closed streamlines in planar flows,” IEEE Transactions on Visualization and Computer Graphics, Vol. 7, No. 2, pp. 165-172, 2001.